A Planar Resonant Sensor for the Complex Permittivity Characterization of Materials

Elisa Fratticcioli, Marco Dionigi, Roberto Sorrentino

D.I.E.I of the University of Perugia, Perugia, via G. Duranti 93, 06125 Perugia, Italy

Abstract — **A microwave planar resonant sensor for the measurement of the complex permittivity in compact areas and thin layers of the material under test (MUT) is presented. Compared to transmission or reflection sensors, the adoption of a scalar 2-port measurement procedure reduces the cost of the system and improves its robustness. Compared to coaxial line sensors, a substantial cost reduction is achieved. The low cost of the sensor allows its use even in a disposable manner. Through the fullwave characterization of the probe a simple equivalent semilumped model of the interaction with the MUT has been derived along with a software calibration procedure. An excellent measurement accuracy in a wide range of complex dielectric permittivities is shown to be feasible.**

I. Introduction

The automation of industrial processes requires the development of advanced sensors for a wide range of measurement applications [1]. A wide category concerns the dielectric properties of materials, for which microwave sensors are widely employed operating either as resonators or as transmission and reflection elements.

Wideband permittivity measurements are basically made by transmission sensors [2] or reflection sensors such as coaxial probes [3]. This kind of measurement is often too complicated for industrial applications. Expensive instrumentations such as vector network analyzers are needed, making this approach inappropriate within industrial environments or for *in situ* measurements.

Sensors requiring merely scalar measurements allow less expensive and more robust instrumentation to be employed. Resonant sensors can be fully described in terms of scalar measurements, so that they lend themselves to industrial applications and *in situ* measurements, whenever wide-band characterization is not required. Physical properties of the materials can then be extracted once the permittivity of the sample has been measured.

A typical application of resonant sensors has been demonstrated in a previous work [4], where a complete system for monitoring the moisture content of wet powered materials has been presented. In such a system, an open-ended coaxial resonator was adopted as the sensing head. Besides requiring a preliminary experimental calibration, the coaxial resonator in unsuited for measuring the moisture content of thin layers as well as in compact areas.

To cover such applications, a novel planar resonant sensor has been developed and is presented in this paper. The new sensing head can directly replace the previous one, thus extending the measurement capability to thin layers and small areas. In addition, by introducing an accurate equivalent circuit model for the planar sensor the experimental calibration procedure is avoided. The low cost and simplicity of manufacturing allows the use of the resonator also in disposable manner.

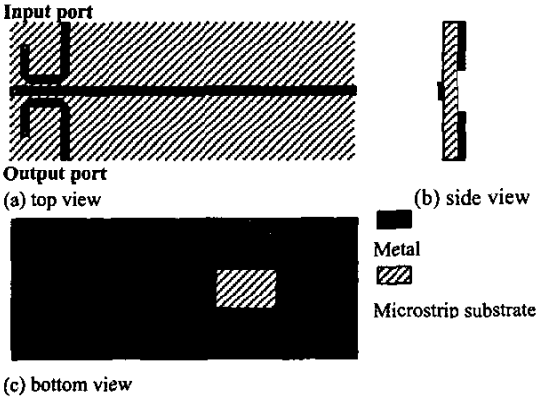

Fig. 1. Geometry of the sensor (not scaled)

II. The Planar Resonant Sensor

The sensor is sketched in Fig. 1. It consists of a quarter wavelength resonant microstrip line with a distributed coupling section to the input and output signal ports. The microstrip line is 70 mm long, open-ended at one end and grounded by a via hole at the other end. The nominal substrate permittivity is $\varepsilon_r = 3.2$, with $tg\delta = 0.003$.

The interaction with the Material Under Test (MUT) occurs through a rectangular slot (10 mm long, 8 mm wide) cut in the ground plane. The distance between the coupled lines in the input/output section is chosen in such a way as to achieve a trade off between the transmitted signal level and the Q factor of the resonator. The coupling is placed at the maximum of current amplitude (near the

0-7803-7239-5/02/$10.00 © 2002 IEEE

via holes). 45° mitered bends are used to minimize unwanted interaction.

The circuit can be analyzed using commercial full-wave simulators based on the Moment Method [5]. The MUT is represented by a sublayer underneath the microstrip ground.

Since the slot in the ground plane is far enough from the input and output ports, the interaction of the MUT with the sensor occurs only in the slotted-ground section of the microstripline. From now on we will concentrate our attention to this part of the circuit.

With the following assumptions [6], [7]:

a) the slotted-ground section can be viewed as a transmission line length with characteristic impedance

$$Z_c = \frac{Z_0}{\sqrt{\varepsilon_{eff}}} \tag{1}$$

where Zo is the caracteristic impedance of the line section when all dielectrics are removed and ε_{eff} is the MUT-dependent effective permittivity of the line.

b) the slot length l is small compared to the wavelength, so that the slotted-ground line section can be approximated by the lumped equivalent circuit of Fig.2.a where:

$$Z = R + j\omega L = Z_c \cdot sinhk\ell \approx Z_c \cdot k\ell \tag{2}$$

$$\frac{Y}{2} = G + j\omega C = Y_c \cdot \tanh\frac{k\ell}{2} \approx Y_c \cdot \frac{k\ell}{2} \tag{3}$$

k being the complex propagation constant of the transmission line.

Let us now assume that the circuit is lossless, so that R=0, G=0. The presence of the losses will be taken into account later on. For a lossless circuit, L and C can be obtained as

$$L = Z_0\sqrt{\mu_0\varepsilon_0}\cdot\ell \tag{4}$$

$$C = \frac{\varepsilon_{eff}}{Z_0}\sqrt{\mu_0\varepsilon_0}\cdot\frac{\ell}{2} = \varepsilon_{eff}\cdot C_0 \tag{5}$$

where Co is the shunt capacitance value when all dielectrics are removed.

To account for the fringing field at the slot edges, two additional capacitors C_f are to be inserted in the equivalent circuit as shown in Fig. 2b. It can be assumed that the fringe capacitance C_f is not affected by the MUT, since the stray electric field at the slot edge is essentially confined to the microsrip substrate. Under the above assumptions, the slotted ground section is represented by a lumped equivalent circuit of Fig 2.bwhere only the capacitor C is affected by the MUT.

The presence of a lossy MUT can be taken into account by two additional conductances G in shunt with the capacitors. The computation of G will be shown in the next Section.

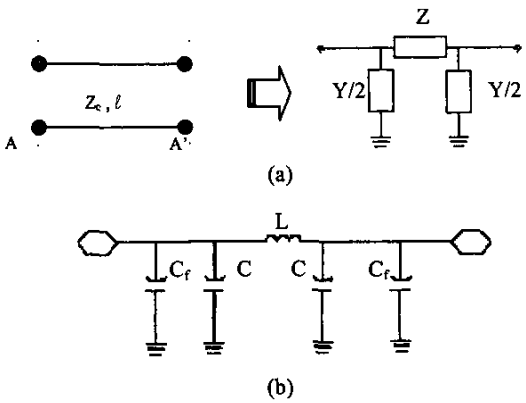

Fig. 2. Equivalent lumped circuit (a), total semilumped subcircuit (b)

III. CALIBRATION

The unknown parameters (L, C. C_f) of the equivalent circuit can be determined using a fitting algorithm by simulating the response of the sensor loaded with known dielectric materials. Since, as seen above, only C is affected by the MUT, L and C_f can be computed using the simulated unloaded response.

Once the C value have been determined, the effective permittivity of the slotted-ground line can be computed from (5). In the quasi static approximation, the effective permittivity can be expressed as a linear combination of the permittivities of the air (ε_r= 1), the substrate (ε'_{SUB}) and the MUT(ε'_{MUT}):

$$\varepsilon_{eff} = q_{MUT}\cdot\varepsilon'_{MUT} + q_{SUB}\cdot\varepsilon'_{SUB} + 1 - q_{MUT} - q_{SUB} \tag{6}$$

q_{MUT} and q_{SUB} being the corresponding filling factors. They are obtained by calculating the fractions of the total energy (volume integral of $\mathbf{E}\cdot\mathbf{E}^*$) stored in the three regions (MUT, substrate and air), [8]. As the values of those integrals can be expressed in terms of the effective permittivity, it can be shown that the filling factors are given by:

$$q_{MUT} = \frac{\varepsilon^{**}_{eff} - \varepsilon^{*}_{eff}}{\varepsilon'_{MUT} - 1}, q_{SUB} = \frac{\varepsilon^{*}_{eff} - 1}{\varepsilon'_{SUB} - 1} \tag{7}$$

where ε^{**}_{eff} is the value in the presence of the MUT, while ε^{*}_{eff} refers to the unloaded case.

Equations (7) show that the MUT filling factor q_{MUT} depends not only on the structure geometry but also on the MUT dielectric constant, while q_{SUB} is independent of the MUT.

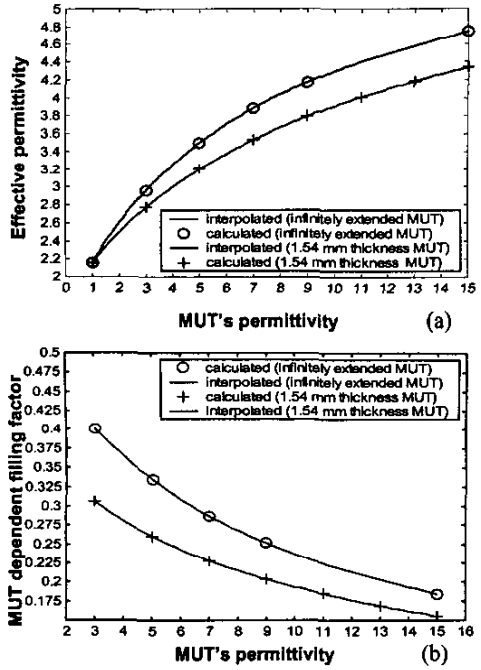

Fig. 3. Calculation of the effective permittivity (a), and q factor (b) of the MUT using spline interpolation

After the calibration with known dielectrics and using spline interpolation, both ε_{eff} and q_{MUT} can be directly calculated as functions of the MUT relative dielectric constant (Fig.3).

Under the same assumptions made for the present case thin layers of different thickness could be considered, leading to a collection of plots like those in Fig.3.As already mentioned, the loss in the MUT, thus the imaginary part ε''_{MUT} of its permittivity, is represented by shunt conductances G in the equivalent circuit of Fig.2. G can be calculated in terms of the shunt capacitance C, under the same assumptions on the total energy distribution [8]. In the present approach the conductance is modeled as follow:

$$G = \left[\left(A(\varepsilon'_{MUT})\varepsilon''_{MUT} + B(\varepsilon'_{MUT})\right)\cdot q1 + \varepsilon''_{SUB}\cdot q2\right]\cdot\omega\cdot C_0 \qquad (8)$$

where: $A(\varepsilon'_{MUT}) = \alpha\cdot\varepsilon'^{\beta}_{MUT}$ and $B(\varepsilon'_{MUT}) = m\cdot\varepsilon'_{MUT} + q$ are empirically chosen allometric and linear functions, respectively. The parameters α, β, m, q are obtained by a four-point fitting on given MUT responses.

Once the calibration procedure has been performed, the whole measuring procedure can be implemented in order to determine the dielectric permittivity of the unknown MUT.

IV. Measurement Procedure

The response of the resonant sensor is identified by the (scalar) measurement of the power transmitted through the ports; the response is sampled at a discrete set of frequencies, then interpolated by Lorentzian fitting. This allows the resonant frequency and the bandwidth to be computed in a fast and accurate way [4].

Forcing the sensor model to exhibit the same resonant frequency as the measured one, the MUT effective permittivity is determined, and by a simple inversion of the previously plotted function the MUT's relative dielectric constant at the resonant frequency is obtained.

Next the MUT's filling factor is computed by (7), leading to the determination of the dielectric losses, thus of the MUT loss tangent.

V. Results

A. Measurement Simulation

The measurement of a material with known dielectric constant has been simulated in order to check the accuracy of the procedure.

The value of the test dielectric constant is 5.5-j0.1925, which leads to a resonant frequency of 656.58 MHz. The data file written by the full wave simulator has been used as if obtained from a measurement device. The value of C that makes the two resonant frequencies match is 0.284 pF, which leads to ε_{eff}=3.6 and ε'_{MUT}=5.495. The comparison of the full-wave simulated response with the lossless model is shown in Fig. 4a. To include the MUT loss in the model, the value of q_{MUT} has then been computed. The additional fitting step leads to the evaluation of G in eqn. (8), thus of unknown ε''. The ε''_{MUT} value obtained is 0.19315 with an error of 0.34%.

The comparison of the simulated response with the lossy model shows an excellent agreement over the entire frequency band (Fig. 4b).

A set of measurement simulations have then been done for different values of relative complex permittivity ($\varepsilon' - j\varepsilon''$) of the MUT.

The results in Tab.1 show that errors in the evaluation of ε' and ε'' are lower than 1% and 2% respectively.

B. Experiments

Four samples of different materials have been measured: the samples where bricks (approximatively 10x2x3 cm) of Teflon, PVC, PEHD (*high density polyethylene),* Nylon.

The results for ε' (Tab.2) have been compared with tabulated values [9], imaginary part has been measured but there is no literature to compare the results with, so measures by resonant sensor have been compared with

those obtained using a HP4291A Impedance Meter and HP16453A Test Fixture (Tab.3).

Excellent agreement has been achieved for the real part of the permittivity, while a larger disagreement has been found on thew imaginary part value. This can be explained by the low accuracy of the HP42921 Impedance Meter for low loss subsrates and by the uncertainty in the imaginary part of the calibration material.

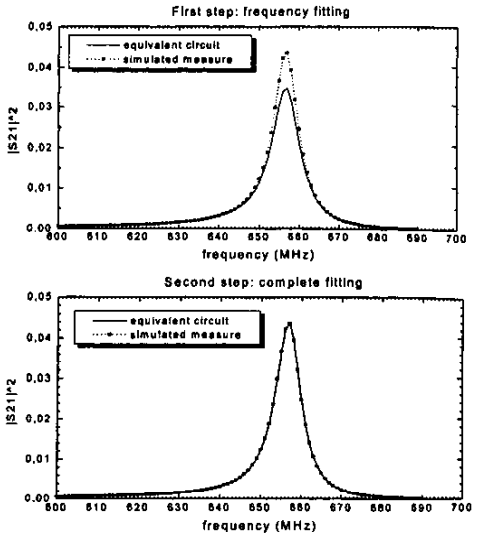

Fig. 4. Comparing the equivalent circuit results to the simulated response after application of fitting algorithm

MUT's permittivity		Calculated permittivity		Error (%)	
ε'	ε"	ε'	ε"	ε'	ε"
5.5	0.044	5.45	0.04447	0.91	1.07
5.5	0.1925	5.495	0.19315	0.18	0.34
5.5	0.495	5.514	0.49973	0.25	0.96
7.3	0.0584	7.251	0.05806	0.67	0.58
7.3	0.2555	7.247	0.2596	0.73	1.60
7.3	0.657	7.36	0.6612	0.82	0.64
9.2	0.0736	9.22	0.0727	0.22	1.22
9.2	0.322	9.16	0.316	0.43	1.86
9.2	0.828	9.265	0.814	0.71	1.69

Tab.1 Simulation of permittivity measurement: results

Sample	Measured [ε' ε"]		Tabulated ε' *
Teflon	2.07	0.0001	2.1
PVC	2.91	0.029	2.8÷2.9
PEHD	2.36	0.004	2,3
Nylon	2.95	0,026	2.8÷3.14

Tab.2 Permittivity measurement: experiment. *See[9]

Sample	Resonant sensor		HP Imped. Meter	
	ε'	ε"	ε'	ε"
PVC	2.91	0.029	2.92	0.0175
PEHD	2.36	0.004	2.38	0.002
Nylon	2.95	0.026	2.97	0.036

Tab.3 Comparing values obtained using our planar resonant sensor and HP4291A Impedance Meter.

VI. CONCLUSIONS

A planar resonant sensor has been developed. The sensor is suitable for measurement of materials permittivity in compact areas and thin layers by scalar 2 port measurements, reducing the cost of the measuring system and improving its robustness. Moreover the low cost of the sensor allows its use even in disposable manner. The fullwave characterization of the probe has led to a simple electrical semilumped model and to a software calibration procedure. The fullwave simulated measurement shows an excellent accuracy in the measurement of the complex dielectric permittivity of the MUT. Experiments confirm a good performance of the planar sensor.

ACKNOWLEDGEMENT

The authors gratefully acknowledge the support of the company Marcantonini Lamberto S.R.L.

REFERENCES

[1] E.Nyfors, P.Vainikainen, *"Industrial Microwave Sensors"*, Norwood, Artech House, 1989.

[2] S.Trabelsi, A.W.Kraszewski, S.O.Nelson, *"New Density-Independent Calibration Function for Microwave sensing of Moisture Content in Particulate Materials"*, IEEE Trans. on Inst. and Meas., vol.47, N°3, June 1998, pp.613-621.

[3] M.A.Stuchly, S.S.Stuchly, *"Coaxial Line Reflection Methods for Measuring Dielectric Properties of Biological Substances at Radio and Microwave Frequencies-A Review"*, IEEE Trans. on Inst. and Meas., vol.29, N°3, September 1980, pp.176-183.

[4] G.Bianchi, M.Dionigi, D.Fioretto, R.Sorrentino, *" A microwave System for Moisture Monitoring in Wet Powders for Industrial Applications"*, IEEE MTT-s International Microwave Symposium Digest, 13-19 June1999 Anaheim CA, pp 1603-1606

[5] ADS Reference Manual, Agilent Technologies, 1999.

[6] G.Matthaei, L.Young, E.M.T. Jones, *"Microwave Filters, Impedance Maching Networks, and Coupling Structures"*, Boston, Artech House, 1980.

[7] K.C.Gupta, R.Garg, I.Bahl, P.Bhartia, *"Microstrip Lines and Slotlines"*, Second Edition, Boston, Artech House.

[8] R. E. Collin, *"Foundations for Microwave Engineering"*, New York, McGraw-Hill, 1992.

[9] D.R. Lide, *"Handbook of Chemistry and Physics"*, CRC Press, 1999, tab.13-12.